

Long lasting low energy thunderstorm ground enhancements and possible Rn-222 daughter isotopes contamination

A. Chilingarian^{1,2,3}

¹*A. Alikhanyan National Lab (Yerevan Physics Institute), Yerevan 0036, Armenia*

²*National Research Nuclear University MEPhI, Moscow 115409, Russia*

³*Space Research Institute of RAS, Moscow 117997, Russia*



(Received 6 May 2018; published 11 July 2018)

Thunderstorm ground enhancements (TGEs) comprise large particle fluxes coming from the clouds that usually coincide with thunderstorms. Most of TGEs observed at the Aragats research station in Armenia during the last ten years originated from “beams of the electron accelerator” operating in the thunderclouds above the research station. Observed TGEs contain high-energy electrons and gamma rays (as well as neutrons) and usually last a few minutes. Starting from 2014, we use particle detectors tuned for the registration of lower energies particles coming from thunderclouds (starting from 0.3 MeV). In 2016, we already noticed that TGEs measured by particle detectors with a low energy threshold demonstrated a drastically larger duration. The flux of the high-energy particles (with energies up to 40 MeV) lasts 1–10 min; the lowest ones (less than 3 MeV)—more than two hours. All intense TGEs contain a high-energy peak and a prolonged low-energy extension lasting 2–3 h. In the presented paper, we describe examples of long-lasting TGEs and discuss correlations of enhanced particle fluxes with disturbances of the electric field and with precipitation.

DOI: [10.1103/PhysRevD.98.022007](https://doi.org/10.1103/PhysRevD.98.022007)

I. INTRODUCTION

The bulk of information on particle fluxes correlated with thunderstorms (thunderstorm ground enhancements, TGEs, [1–3]) can be used to better understand the electrical structure of thunderclouds and high-energy processes in the atmosphere. In the strong intracloud electric fields, seed electrons from the ambient population of secondary cosmic rays gain such an amount of energy that they surpass the electron energy losses and “run away”, giving rise to electron-photon avalanches. Thus, the bulk of runaway electrons and gamma rays results in a runaway breakdown (RB, [4]), recently referred to as a relativistic runaway electron avalanche (RREA, [5–7]).

In the last decade, TGEs were investigated at the Aragats research station of the Yerevan Physics Institute. The Aragats research station is located at an altitude of 3200 m on the plateau near a large lake, and the height of the cloud base above the ground is typically 25–50 m in spring, increasing to 100–200 m in the summer. In the 2017–2018 campaigns on Aragats, we paid special attention to the long lasting low energy TGEs (LLL TGE). NaI spectrometers and large area plastic scintillators were used to detect enhanced fluxes of low energy fluxes (less than 3 MeV) of gamma rays. A concern is that it is very important to distinguish particle avalanches initiated by runaway electrons, from the radiation of environmental isotopes; those fluxes are also possibly increased during a thunderstorm [8,9].

Analysis of TGE data allows us to associate the particle flux enhancement with the acceleration of electrons in the strong electric fields emerging in a thundercloud [10]. However, even without noticeable disturbances of the near surface electric field, the flux of the low energy gamma rays is observed. We relate this phenomenon to the detection of Compton scattered gamma rays from remote electron-gamma ray cascades and/or randomly emerging small size stochastic electric fields above the detector site [11].

Neutral and charged particle fluxes are measured on Aragats with various elementary particle detectors. Count rates are measured with plastic scintillators, proportional chambers, and NaI and CsI crystals on the time scale from tens of nanoseconds to minutes. Energy release histograms are measured each minute with NaI crystals and each 20 s with 60-cm thick plastic scintillators. Energy release histograms are transformed to differential energy spectra using a detector response function calculated by GEANT simulations. Details of the particle detector operation and spectra deconvolution can be found in [12]. We also measure the near-surface electrostatic field with four electric field mills EFM-100 produced by the Boltek company. The stormy weather is usually accompanied by precipitation that possibly brings the radioactive isotopes, lightning flashes, strong wind, and fast changes of the atmospheric pressure. Abrupt decrease of atmospheric pressure can also increase the flux of most species of cosmic rays (although not exceeding $\sim -0.5\%/mb$).

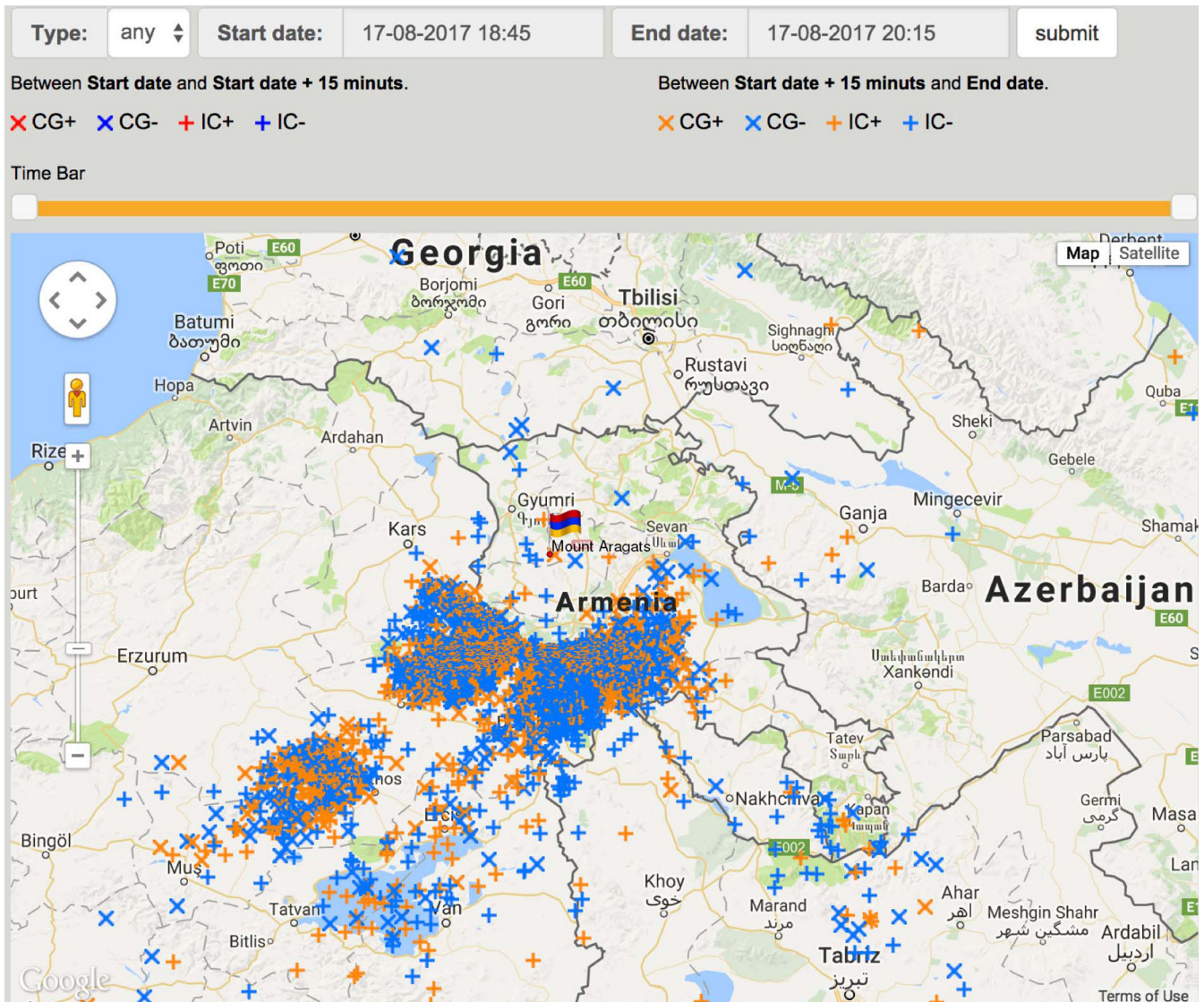


FIG. 1. Pattern of the storm in Armenia mapped by lightning flashes showing the approaching storm front; the Aragats station position on the map is flagged.

Thus, several meteorological factors can be responsible for the measured enhancements of the particle flux. One of the goals of this paper is to find out which of these factors is responsible for the long-lasting TGEs. That is why, in addition to the particle flux measurements, we are continuously monitoring a set of meteorological parameters with the Professional Davis Instruments Vantage Pro2 weather station (<http://www.davisnet.com/>). Also, we trace the evolution of the stormy weather on Aragats by mapping the approaching storm front with a sequence of atmospheric flashes registered by the lightning detector of the Boltek company (Boltek's StormTracker Lightning Detection System, powered by the software from Astrogenic systems, <http://www.boltek.com/stormtracker>).

The wideband fast electric field is measured by three circular flat plate antennas attached to fast digital oscilloscopes, which are triggered by the signal from active whip

antennas [13]. The oscilloscopes are also used to monitor signals from particle detectors. In our first papers on TGE measurements [1,2,14,15], we used particle detectors from the MAKET surface array [16], registering the electron content of extensive air showers (EAS). The energy threshold of these detectors was ~ 7 MeV, suitable for the EAS research. In the presented paper, we analyze measurements obtained with particle detectors having a significantly smaller energy threshold of ~ 0.3 MeV and ~ 0.7 MeV that allows us to discover new important features of TGE.

II. DETAILED ANALYSIS OF THE SUMMER TGE EVENT OCCURRED ON AUGUST 17, 2017

August 2017 was very stormy on Aragats with numerous lightning flashes, and the first snow appeared on mountain

peaks. On August 17, 2017, a storm started as usual in the Armenian highlands in Turkey, southwest from Aragats, and rapidly moved to Armenia’s border, see Fig. 1. The meteorological environments on August 17, 2017 changed abruptly as the storm reached Aragats, see Fig. 2, where we show in the top of the picture the outside temperature and dew point, the rain rate in the bottom, and atmospheric pressure and disturbances of the near surface electric field in the middle. The height of the cloud is estimated by the measured “spread” parameter—the difference between the air temperature and the dew point. The calculation of the height of cloud base is based on the assumption that the air temperature drops 9.84 °C per 1000 m of altitude and the dew point drops 1.82 °C per 1000 meters’ altitude.

There are several WEB calculators for the estimation of the altitude of a cloud (see, for instance, <http://www.csgnetwork.com/cloudaltcalc.html>). The simplified estimate consists in multiplying the spread measured in °C by 122 m. With this approach, we estimate the height of cloud before the start of the storm to be $(9.1-6.0) * 122 \sim 400$ m; sharply decreased to ~ 130 m on the start of the storm $(7.0 - 5.9) * 122$. Relative humidity also increased from 81% up to 92%, which signaled the decreasing of the height of the cloud base. During the spring storms when clouds were “sitting” on the station, the height of cloud base was 25–50 m and RH 96%–98%.

Atmospheric pressure increased from 694.8 at 18:40 up to 695.9 at 18:58 and back to 684.9 at 20:10,

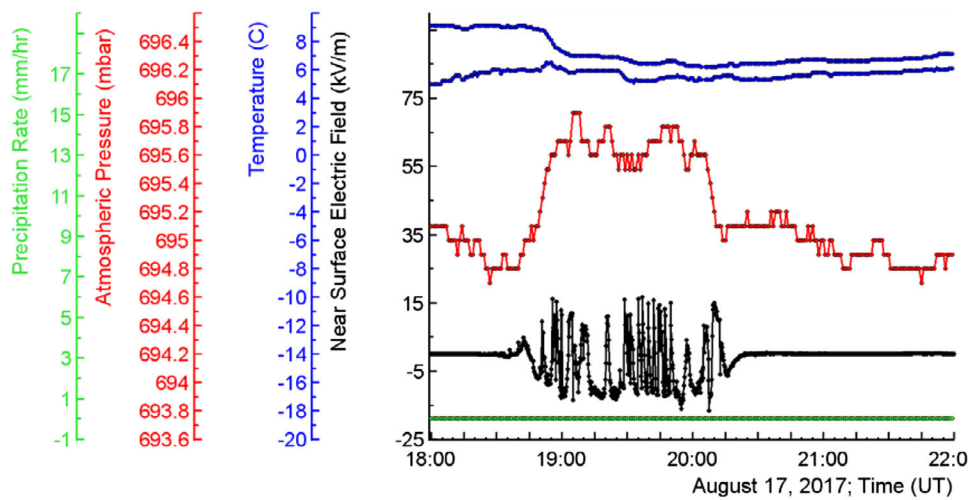


FIG. 2. Meteorological parameters measured on August 17, 2017. On the top of the picture, one-minute time series of the outside temperature and dew point are shown; in the middle—the atmospheric pressure and the disturbances of electric field; in the bottom—the rain rate.

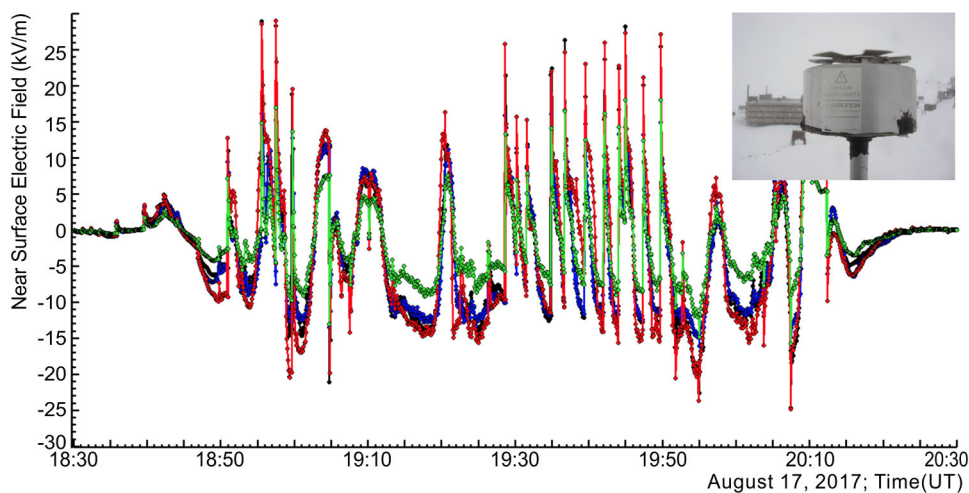


FIG. 3. The lightning activity during a large summer storm on Aragats was coherently detected by the network of the four electric mills EFM-100 of the Boltek company (see inset in the top right corner of the picture).

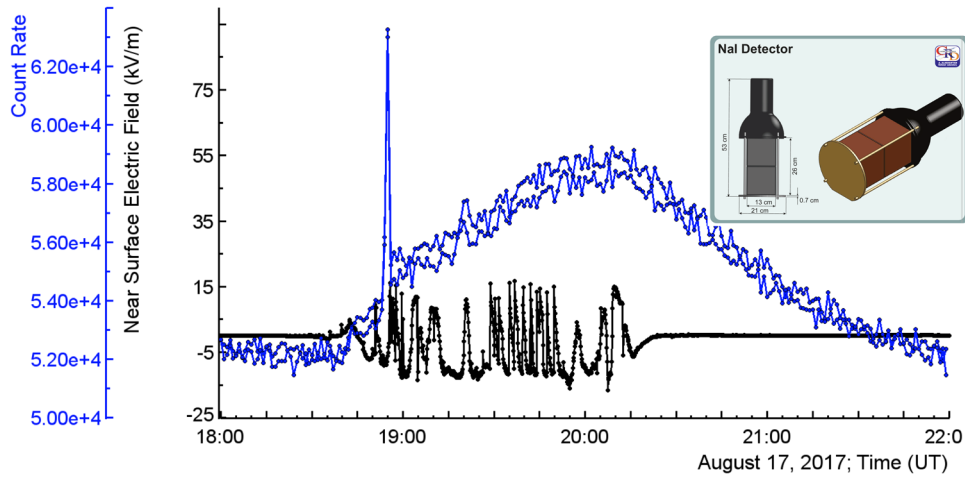


FIG. 4. Thunderstorm ground enhancement (TGE) as measured by the first and second crystals of the NaI network (see inset, energy threshold 0.3 MeV).

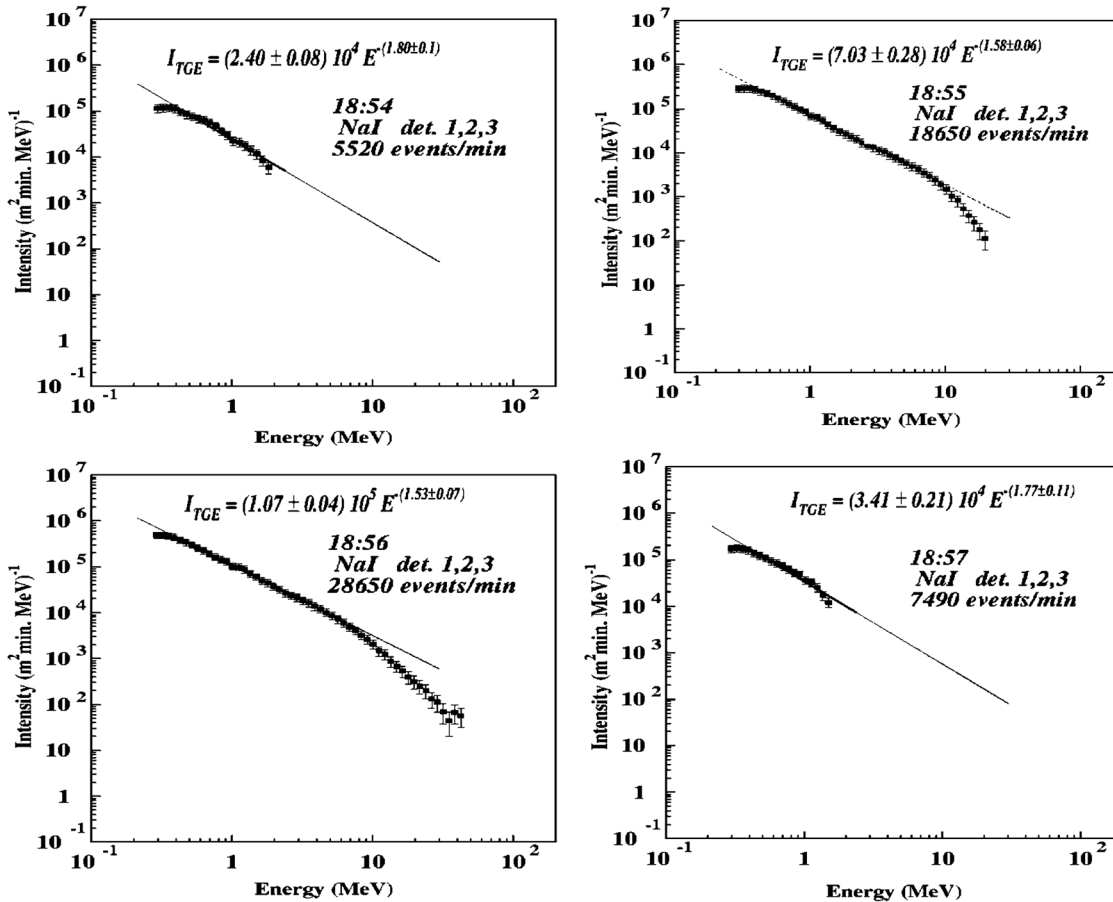


FIG. 5. The differential energy spectra of four subsequent minutes of TGE, recovered from the energy release histograms measured by the N1 and N2 crystals of the NaI network.

precisely coinciding in time with the disturbances of the near-surface electric field (from -25 to 30 kV/m) measured by the electric mill located on the roof of the MAKET experimental hall. No rainfall was detected

by the Davis weather station located in the same place.

The storm started on Aragats at 18:36; the near-surface electric field remained disturbed for 1 h 42 min until 20:20,

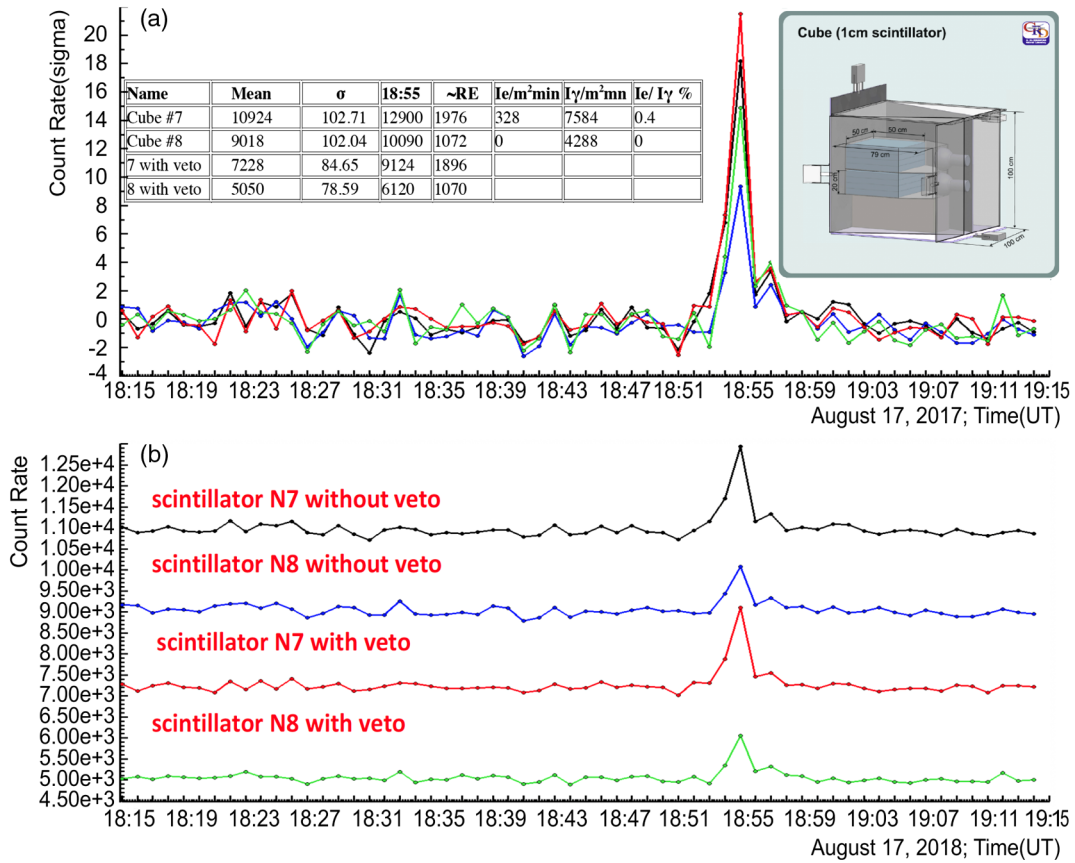


FIG. 6. Recovery of gamma rays and electron fluxes with the CUBE detector. Scintillators N7 and N8 are 20 cm thick 0.25 m² stacked plastics. In the Table inset, the recovered fluxes measured by both thick scintillators are shown.

see Fig. 2. The storm was accompanied with numerous lightning flashes (which produced abrupt changes of the electrostatic field of positive and negative polarity) detected by all four electric mills located on the Aragats station, see Fig. 3.

The rise of the particle flux measured by large NaI crystals (12.5 × 25 cm, energy threshold 0.3 MeV, see inset in Fig. 4) started at 18:40; after 13 min there occurred a 2-min long huge burst of particles coming from the cloud. At 18:55–18:56, the flux enhancement was 120%, corresponding to 43 standard deviations from the flux mean value measured before TGE. At 19:00–21:00, the particle flux enhancement was 3%–10%. In Fig. 4, we see that after the short burst, the particle flux continued to rise until the disturbances finished at ~20:20. After the storm calmed down at ~20:20, the flux started to decay and finally declined at ~22:00. Thus, the enhanced flux continued for ~2.5 h and during the last hour—without any detectable disturbance of the electric field.

From Fig. 2, it is obvious that precipitation plays no role in this TGE origination. As there was no rain through the ~4-h duration of the TGE, we cannot connect the enhanced flux with the Radon daughter’s decays. The observed enhancement of the atmospheric pressure also cannot explain the TGE: the change of 1 mb can lead only to

an ~0.5% enhancement of the gamma ray flux, and only if the atmospheric pressure is decreasing and not increasing as we see in Fig. 2.

Also, we can notice that the flux enhancement coincides with disturbances of the electric field (a proxy of the intracloud electric field) and with a low location of the cloud base. According to the standard TGE model [17,18], the main negatively charged region with the emerged lower positively charged region (LPCR) formed a dipole which accelerates cosmic ray electrons downwards to the particle detectors located on the Earth’s surface. If the electric field is strong enough, a RREA process is unleashed resulting in the large TGE. The explanation of the TGE decay phase that started at 20:20 in the absence of disturbances of the electric field needs additional simulation and experimental efforts and will be discussed in the Conclusions section.

In Fig. 5, we show the energy spectra of the TGE measured during the particle burst and just before and after it. The energy release histograms were measured with the same NaI crystals (N1 and N2); those count rates are posted in the Fig. 4. The differential energy spectra were recovered taking into account the spectrometer’s response function for each of NaI crystal (see, for details, the supplement to [12]).

As we can see in Fig. 5, for 2 min only, the particle flux contains particles with energies up to 40 MeV. We identify

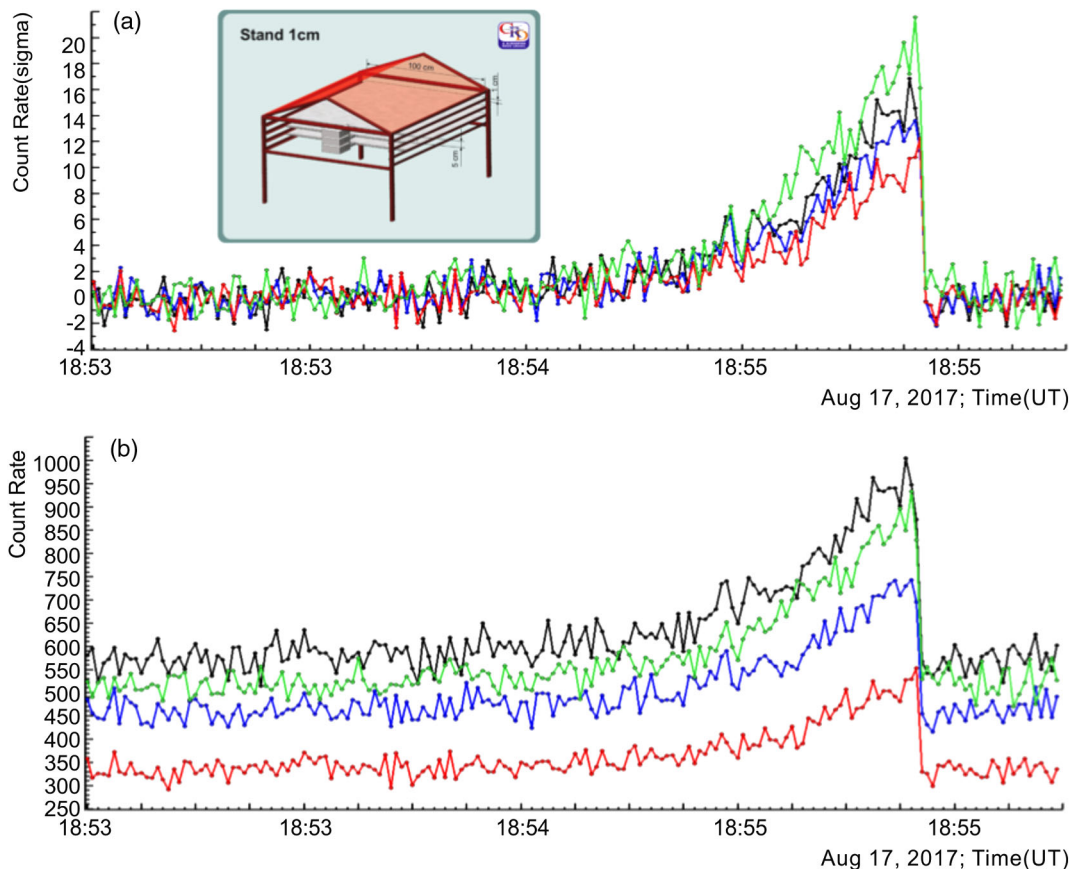


FIG. 7. One-second count rates of the STAND1 detector located nearby the MAKET experimental hall.

the high-energy particle flux with the RB/RRE avalanches released just above the particle detectors site. After the avalanche process stopped (or moved away), the energy spectra resumed to the lower energies, not exceeding few MeV. The cover of the NaI crystals stopped the electrons with energies below ~ 3 MeV; thus, the particle registered by the NaI spectrometers before and after the 2-min burst were gamma rays only.

The RB/RREA cascade after leaving the lower dipole propagates in the air and, depending on the cloud height, the fraction of the electrons reaching the Earth's surface will dramatically change due to a much larger attenuation of electrons (see Fig. 19 of [14]). Usually, the RB/RREA flux as measured on the Earth's surface consists mostly of gamma rays contaminated by a small fraction of electrons. To estimate the electron fraction, we use a CUBE detector (inset in Fig. 6; see, for details, the supplement of [12]).

The CUBE detector consists of two stacked 20 cm thick plastic scintillators of a 0.25 m^2 area surrounded by the "veto" that consists of six 1 cm thick and 1 m^2 area plastic scintillators. A CUBE detector registered 1-min count rates of all eight scintillators and counts of the inner thick scintillators under the condition of the absence of an electronic signal from anticoincidence shielding. Because the 1 cm thick scintillators have a nonzero probability to miss the registration of a charged particle as well as to register a neutral particle, we develop a special method to estimate "true" intensities (integral energy spectra) of gamma ray and electron fluxes (see Appendix A of [14]). In Fig. 6(b), we show the count rates of thick scintillators with and without the veto option. In Fig. 6(a), we show the same count rates but in the units of standard deviation (the number of). In the inserted table, we show the mean values of the count rates and variances before a particle burst and

TABLE I. The characteristics of short burst of high-energy particles occurred on August 17, 2017.

Name	Mean	σ	18:55:33	Sign. peak $N\sigma$	% of drop
STAND1 MAKET Ch. 1	571.4	25.4	1002	17	76
STAND1 MAKET Ch. 2	456.3	22.7	741	14	62
STAND1 MAKET Ch. 3	329.7	18.1	553	12	67
STAND1 MAKET Ch. 4	510.9	22.3	932	21	75

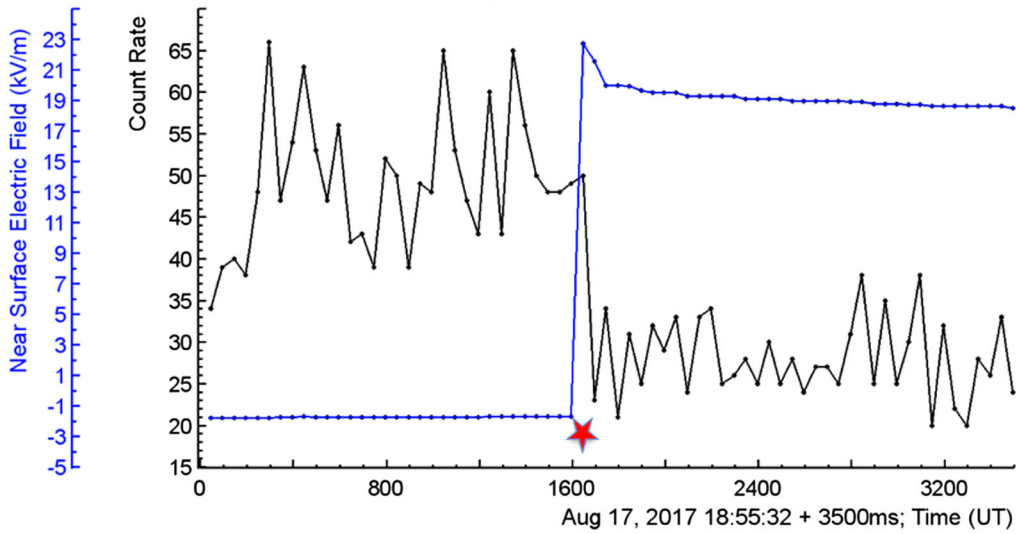


FIG. 8. The 50-ms time series of the STAN1 upper scintillator count rate (located outdoors nearby the MAKET experimental hall) and of the near surface electric field measurements. The asterisk indicates the time of lightning flash registered by the World-Wide Lightning Location Network (WWLLN, detection at 18:55:33.630). The horizontal axes started from 18:55:32; each tick on the axes corresponds to 100 ms.

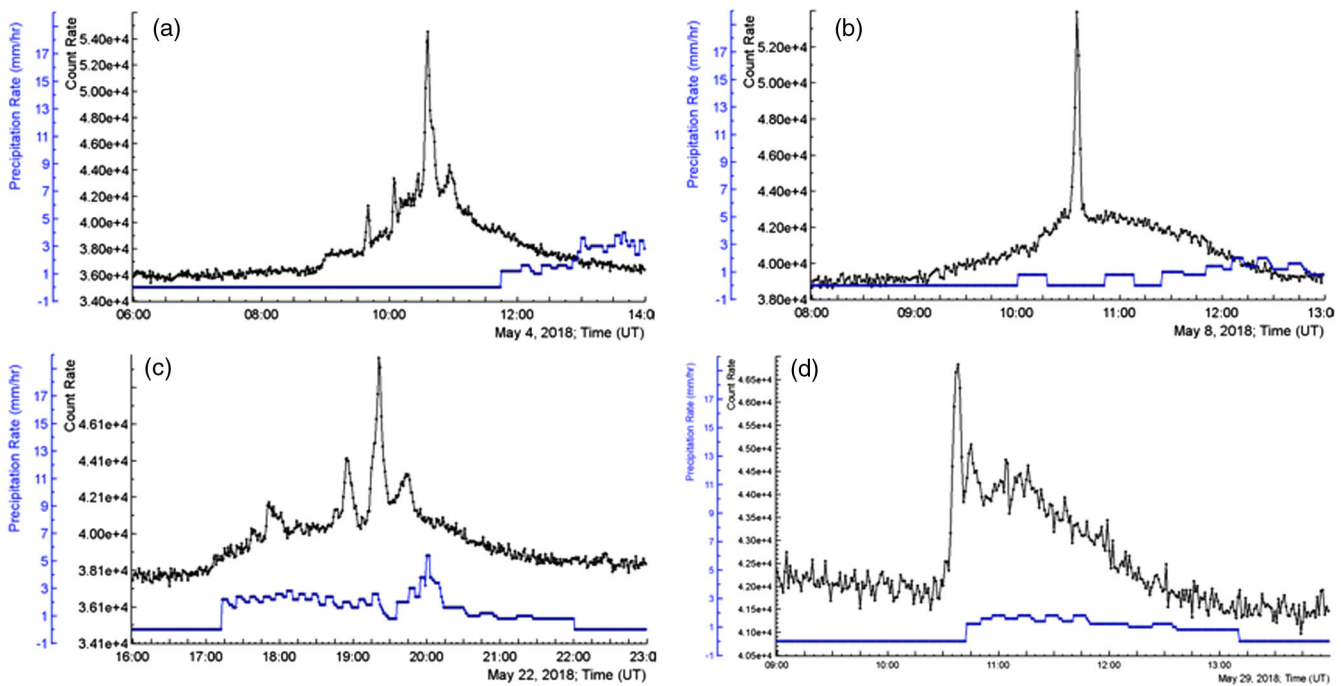


FIG. 9. One-minute time series of the count rates of the 1 cm thick 1 m² area plastic scintillator. In the bottom of the frames, we show rain rate in mm per hour.

during the minute of maximal flux, recovered intensities, and electron fractions for both inner 20 cm thick scintillators. The energy thresholds of thick scintillators are estimated to be 5.8 and 6.4 MeV (scintillator N7 is above N8, see Table 1 in [19]). For a lower energy threshold (scintillator N7), the electron contamination is ~4% and vanishing at higher energies (scintillator N8).

To understand the dynamics of TGE and to investigate the relation of the particle fluxes and lightning flashes, we need to register the time series of the TGEs and electric field disturbances in much more detail. Fast electronics provide the registration of TGEs on time scales of 1 sec and 50 ms, compatible with the fast processes in thunderstorm atmospheres. In Figs. 7 and 8, we demonstrate the

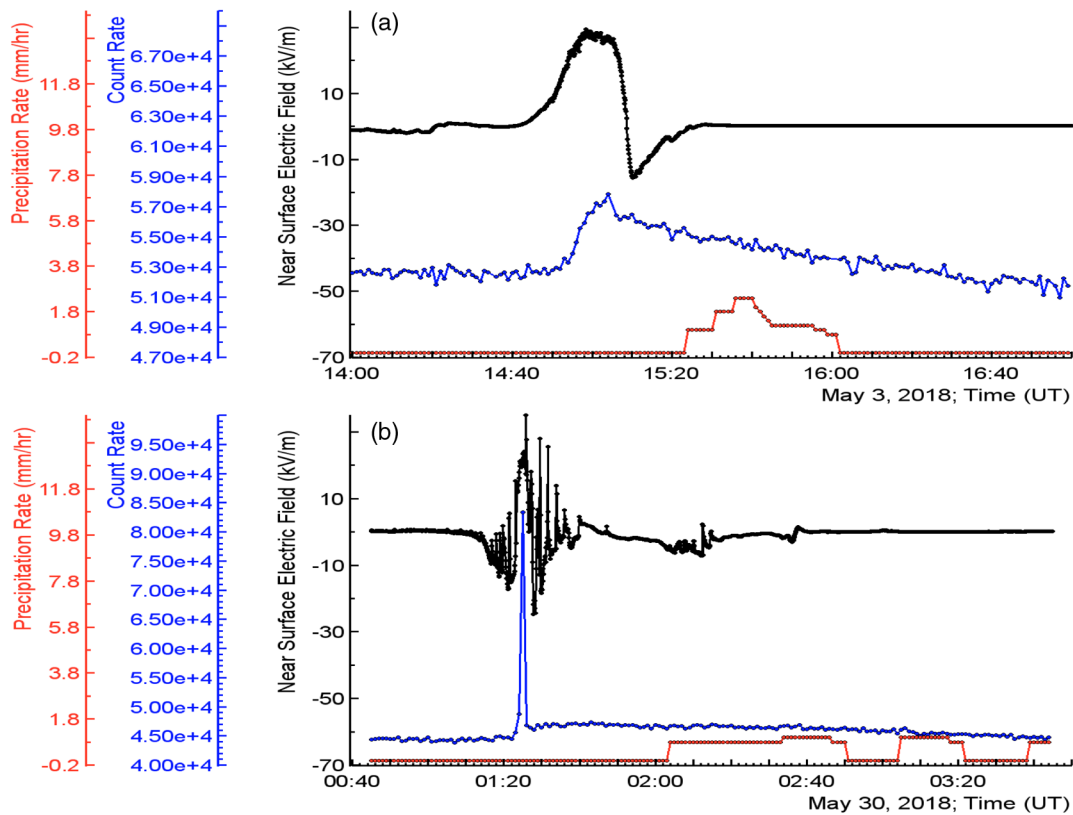


FIG. 10. TGE events registered by the NaI detector. In the top of figures, we show disturbances of the near surface electric field; in the bottom—the rain rate. In the middle—the one-minute count rate of the NaI detector.

possibilities of TGE and lightning analysis at these time scales. The abrupt decay of the TGE is better shown in the one-second time series of the STAND1 detector shown in Fig. 7. The network of the STAND1 detectors comprises three identical units located on Aragats station, each of which consists of three stacked 1 cm thick and 1 m² area plastic scintillators and one stand-alone 3 cm thick plastic scintillator of the same type (inset in Fig. 7; see, for details, the supplement of [12]).

In Fig. 7(b), we show the one-second count rates of the stacked and stand-alone scintillators. In Fig. 7(a), we show the same count rates, but plotted in units of the standard deviations from the mean value measured just before the TGE. In Table 1, we demonstrate the numerical values, significances of peaks (in), and count rate drops for each scintillator. The sharp decay of particle flux that occurred at 18:55:33 is enforced by a lightning flash which stopped the RB/RREA process in the cloud [20,13]. In [21], we demonstrate that strong particle fluxes usually precede lightning flashes.

For the in-depth research of the lightning-particle flux relations, we use a fast data acquisition system based on the National Instruments myRIO board, which produced the GPS time stamp of the record and provided registration of the 50 ms time series of detector count rates (see details in [22]).

In Fig. 8, we can see that the rearrangement of the electric field started at 18:55:33.600. The near surface electric field of -1.6 kV/m after 50 ms reached a value of 22 kV/m, i.e., the amplitude was ~ 23.6 kV/m. The abrupt decay of the particle flux started at the same time; the flux decreased from 50 to 23 particles, i.e., by 54% in 50 ms. This flash was registered by the World-Wide Lightning Location Network (WWLLN, detection at 18:55:33.630).

III. LONG LASTING TGES AND RAINFALLS

In Fig. 9, we summarize typical shapes of TGEs observed in May 2018, when an especially rich harvest of TGEs was collected. We consider only TGEs accompanied with rainfall to examine its possible influence on the particle flux. The one-minute time series of count rates were measured by a 1 cm thick 1 m² area plastic scintillator (energy threshold ~ 0.7 MeV, [19], Fig. 10, Table 1) located outdoor nearby the MAKET experimental hall; the rain rate was measured by the Davis weather station located on the roof of the same building.

Displayed TGEs contain a high-energy part (sharp peaks—gamma rays and electrons with energies up to ~ 40 MeV) lasting a few minutes and a low-energy part (gamma rays below 3 MeV) lasting several hours; see an example of the energy spectra in Fig. 5. In Fig. 9, we can see that TGEs are not connected with rainfall. In Fig. 9(a),

the rain started only at the end of the TGE; in Figs. 9(b), 9(c), and 9(d) strengthening of the rainfall coincides with the decay phase of the TGE. Many other TGEs were not accompanied with rain at all. The TGEs of May 2018 occurred at a highly disturbed near-surface electric field. For the clarity of the displayed information, we do not post the time series of the near surface electric field in Fig. 9 (it is similar to one shown in Fig. 4).

In Fig. 10, we show the count rate enhancement, disturbances of the near-surface electric field, and the rain rate of two TGE events that occurred in the May 2018. The May 3, 2018 event [Fig. 10(a)] is rather small: $\sim 10\%$ enhancement of the count rate of the NaI detector. Rainfall that started after the TGE reached the maximum did not influence the count rate; the decay of the TGE continued. A large event ($\sim 100\%$ count rate enhancement) occurred on May 30, 2018 [Fig. 10(b)], again accompanied by a rainfall at the decay phase of TGE. For both TGEs, rain apparently does not influence the count rate. The atmospheric pressure was not strongly disturbed during both events; the fluctuation does not exceed 1 mb. Thus, we can connect the initiation of a TGE only with disturbances of the electric field and not with precipitation or atmospheric pressure variations.

IV. CONCLUSIONS

Each year, Aragats facilities register more than 100 TGEs, proving that Mount Aragats is a stable electron accelerator for atmospheric high-energy physics research [23]. TGEs varied significantly in intensity and continuation; nonetheless, we can outline some important features confirming Aragats 10-year observations [1,14,18]:

- (i) TGEs occurred during strong storms approaching Armenia mostly from the Armenian highlands in Turkey, southwest from Aragats, which disturbed the near surface electric field at a particle detector location.
- (ii) A strong TGE started with a low energy flux (less than 3 MeV), turning to a short (1–10 min) and intense peak containing high-energy particles (up to 40 MeV).

- (iii) After an abrupt decline of the high-energy part of the TGE, usually forced by a lightning flash, the low-energy flux continued with a prolonged decay. Thus, we detected a sizable flux of gamma rays during the hours of the “fair weather” when the near surface electric field was not disturbed.
- (iv) The radioactive decay from radon isotopes contained in the rain, as well as the variations of atmospheric pressure (barometric effect) are not the cause of TGEs.

There are two main hypotheses about the origin of the prolonged gamma ray flux in the absence of sizable disturbances of the near-surface electric field:

- (i) TGEs originated in the thunderstorm atmospheres due to an emerging strong electric field between differently charged layers in the clouds [14,18,24]. Seed electrons from the ambient population of secondary cosmic rays “run away” [4], accelerated, and form electron-gamma ray avalanches reaching and detected at the Earth’s surface. If the cloud with a strong electric dipole inside migrates from the detector site, Compton scattered gamma rays can reach the detector under large zenith angles and be registered for an extended time span.
- (ii) Small-scale stochastic electric fields randomly emerging in a thundercloud accelerate electrons and enhance the probability of bremsstrahlung radiation and boosts the low energy gamma ray flux.

ACKNOWLEDGEMENTS

The detailed analysis of these scenarios will be presented in our next publication. The data for this paper are available via the multivariate visualization software ADEI on the WEB page of the Cosmic Ray Division (CRD) of the Yerevan Physics Institute in Ref. [25]. Author thanks the staff of the Aragats Space Environmental Center for the uninterrupted operation of Aragats research station facilities. Author thanks Hovsepian Gagik for recovering the energy spectra posted in Fig. 5 and M. Panasuk and V. Bogomolov for useful discussions. Author received support from the Russian Science Foundation grant (Project No. 17-12-01439).

[1] A. Chilingarian, A. Daryan, K. Arakelyan, A. Hovhannisyanyan, B. Mailyan, L. Melkumyan, G. Hovsepyan, S. Chilingaryan, A. Reymers, and L. Vanyan, Ground-based observations of thunderstorm-correlated fluxes of high-energy electrons, gamma rays, and neutrons, *Phys. Rev. D* **82**, 043009 (2010).
 [2] A. Chilingarian, G. Hovsepyan, and A. Hovhannisyanyan, Particle bursts from thunderclouds: Natural particle accelerators above our heads, *Phys. Rev. D* **83**, 062001 (2011).

[3] A. Chilingarian, G. Hovsepyan, and E. Mantasakanyan, Mount Aragats as a stable electron accelerator for atmospheric high-energy physics research, *Phys. Rev. D* **93**, 052006 (2016).
 [4] A. V. Gurevich, G. M. Milikh, and R. A. Roussel-Dupre, Runaway electron mechanism of air breakdown and preconditioning during a thunderstorm. *Phys. Lett.* **165A**, 463 (1992).

- [5] J. R. Dwyer, A fundamental limit on electric fields in air, *Geophys. Res. Lett.* **30**, 2055 (2003).
- [6] L. P. Babich, E. N. Donskoy, R. I. Il'kaev, I. M. Kutsyk, and R. A. Roussel-Dupre, Fundamental parameters of a relativistic runaway electron avalanche in air, *Plasma Phys. Rep.* **30**, 616 (2004).
- [7] V. V. Alexeenko, N. S. Khaerdinov, A. S. Lidvansky, and V. B. Petkov, Transient variations of secondary cosmic rays due to atmospheric electric field and evidence for pre-lightning particle acceleration, *Phys. Lett. A* **301**, 299 (2002).
- [8] F. Fabró, J. Montanyà, N. Pineda, J. Montanyà, N. Pineda, O. Argemí, O. A. van der Velde, D. Romero, and S. Soula, Analysis of energetic radiation associated with thunderstorms in the Ebro delta region in Spain, *J. Geophys. Res. Atmos.* **121**, 9879 (2016).
- [9] V. Bogomolov, A. Chilingarian, G. Garipov *et al.*, Study of TGEs and gamma-flashes from thunderstorms in 20–3000 keV energy range with SINP MSU gamma-ray spectrometers, *Proceedings of 6-th TEPA Symposium*, p. 50, Nor Amberd, 2015 (Tigran Mets, Yerevan, 2015); http://www.iaea.org/inis/collection/NCLCollectionStore/_Public/48/037/48037534.pdf.
- [10] A. Chilingarian, G. Hovsepyan, and L. Vanyan, On the origin of the particle fluxes from the thunderclouds: Energy spectra analysis, *Europhys. Lett.* **106**, 59001 (2014).
- [11] D. I. Iudin Lightning initiation as a noise induced kinetic transition, *Radiophys. Quantum Electron.* **60**, 374 (2017).
- [12] A. Chilingarian, G. Hovsepyan, and B. Mailyan, In situ measurements of the runaway breakdown (RB) on Aragats mountain, *Nucl. Instrum. Methods Phys. Res., Sect. A* **874**, 19 (2017).
- [13] A. Chilingarian, Y. Khanikyants, E. Mareev, D. Pokhsroryan, V. A. Rakov, and S. Soghomonyan, Types of lightning discharges that abruptly terminate enhanced fluxes of energetic radiation and particles observed at ground level, *J. Geophys. Res. Atmos.* **122**, 7582 (2017).
- [14] A. Chilingarian, B. Mailyan, and L. Vanyan, Recovering of the energy spectra of electrons and gamma rays coming from the thunderclouds, *Atmos. Res.* **114–115**, 1 (2012).
- [15] A. Chilingarian, G. Hovsepyan, and L. Kozliner, Thunderstorm ground enhancements: Gamma ray differential energy spectra, *Phys. Rev. D* **88**, 073001 (2013).
- [16] A. Chilingarian, G. Gharagozyan, S. Ghazaryan, G. Hovsepyan, E. Mamidjanyan, L. Melkumyan, V. Romakhin, A. Vardanyan, and S. Sokhoyan, Study of extensive air showers and primary energy spectra by MAKET-ANI detector on mountain Aragats, *Astropart. Phys.* **28**, 58 (2007).
- [17] A. Chilingarian and H. Mkrtchyan, Role of the lower positive charge region (LPCR) in initiation of the thunderstorm ground enhancements (TGEs), *Phys. Rev. D* **86**, 072003 (2012).
- [18] A. Chilingarian, Thunderstorm ground enhancements—Model and relation to lightning flashes, *J. Atmos. Terr. Phys.* **107**, 68 (2014).
- [19] A. Chilingarian, S. Chilingaryan, and G. Hovsepyan, Calibration of particle detectors for secondary cosmic rays using gamma-ray beams from thunderclouds, *Astropart. Phys.* **69**, 37 (2015).
- [20] A. Chilingarian, S. Chilingaryan, and A. Reymers, Atmospheric discharges and particle fluxes, *J. Geophys. Res.* **120**, 5845 (2015).
- [21] A. Chilingarian, S. Chilingaryan, T. Karapetyan, L. Kozliner, Y. Khanikyants, G. Hovsepyan, D. Pokhsroryan, and S. Soghomonyan, On the initiation of lightning in thunderclouds, *Sci. Rep.* **7**, 1371 (2017).
- [22] D. Pokhsroryan, Fast data acquisition system based on NI-myRIO board with GPS time stamping capabilities for atmospheric electricity research, *Proceedings of TEPA 2015* (Nor Amberd, Tigran Mets, 2015), p. 23.
- [23] A. Chilingarian, G. Hovsepyan, and L. Kozliner, Extensive air showers, lightning, and thunderstorm ground enhancements, *Astropart. Phys.* **82**, 21 (2016).
- [24] K. Kudela, J. Chum, M. Kollárik *et al.*, Correlations between secondary cosmic ray rates and strong electric fields at Lomnický štít, *J. Geophys. Res.* **122**, 70010 (2017).
- [25] <http://adei.crd.yerphi.am/adei>.